AD-A043 122   BALLISTIC RESEARCH LABS ABERDEEN PROVING GROUND MD   F/G 12/1
COMMENTS ON THE SOLUTION COUPLED STIFF DIFFERENTIAL EQUATIONS.(U)
JUL 77   M D KREGEL, J M HEIMERL
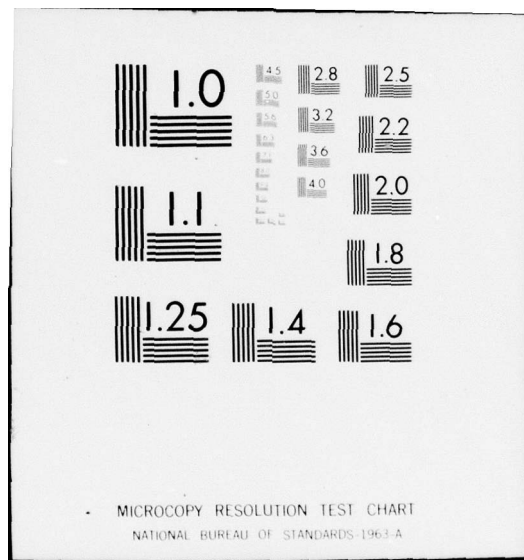
UNCLASSIFIED   BRL-MR-2769   NL

1 OF 1
ADA043122

BRL

END
DATE
FILMED
9-77
DDC

MICROCOPY RESOLUTION TEST CHART

NATIONAL BUREAU OF STANDARDS-1963-A

BRL

AD

MEMORANDUM REPORT NO. 2769

COMMENTS ON THE SOLUTION OF COUPLED
STIFF DIFFERENTIAL EQUATIONS

M. D. Kregel
J. M. Heimerl

July 1977

DDC
AUG 23 1977

USA ARMAMENT RESEARCH AND DEVELOPMENT COMMAND
USA BALLISTIC RESEARCH LABORATORY
ABERDEEN PROVING GROUND, MARYLAND

REPORT DOCUMENTATION PAGE	READ INSTRUCTIONS BEFORE COMPLETING FORM

1. REPORT NUMBER	2. GOVT ACCESSION NO.	3. RECIPIENT'S CATALOG NUMBER
BRL Memorandum Report No. 2769		

4. TITLE *(and Subtitle)*	5. TYPE OF REPORT & PERIOD COVERED
COMMENTS ON THE SOLUTION OF COUPLED STIFF DIFFERENTIAL EQUATIONS	Final
	6. PERFORMING ORG. REPORT NUMBER

7. AUTHOR(s)	8. CONTRACT OR GRANT NUMBER(s)
M. D. Kregel and J. M. Heimerl	

9. PERFORMING ORGANIZATION NAME AND ADDRESS	10. PROGRAM ELEMENT, PROJECT, TASK AREA & WORK UNIT NUMBERS
US Army Ballistic Research Laboratory Aberdeen Proving Ground, Maryland 21005	1L161102AH43, and 1L161102B53A

11. CONTROLLING OFFICE NAME AND ADDRESS	12. REPORT DATE
US Army Materiel Development & Readiness Command 5001 Eisenhower Avenue Alexandria, Virginia 22333	JULY 1977
	13. NUMBER OF PAGES
	23

14. MONITORING AGENCY NAME & ADDRESS*(if different from Controlling Office)*	15. SECURITY CLASS. *(of this report)*
	Unclassified
	15a. DECLASSIFICATION/DOWNGRADING SCHEDULE

16. DISTRIBUTION STATEMENT *(of this Report)*

Approved for public release; distribution unlimited.

17. DISTRIBUTION STATEMENT *(of the abstract entered in Block 20, if different from Report)*

18. SUPPLEMENTARY NOTES

19. KEY WORDS *(Continue on reverse side if necessary and identify by block number)*

K-method integration	Integration algorithm
Variable step size	Stiff differential equations
Predictor-corrector method	Ordinary differential equations
Discontinuous driving functions	

20. ABSTRACT *(Continue on reverse side if necessary and identify by block number)* (eal)
The K-method of integrating sets of ordinary differential equations is outlined. This algorithm employs a variable step size, third order predictor-corrector method. It is written to reduce truncation error and to maximize stability consistent with reasonable execution time. The K-method has been used to integrate equations with discontinuous driving functions and this algorithm conserves chemical balance within the machine round-off error. It has been applied to solve kinetics problems in aeronomy and examples are taken from that field.

DD FORM 1 JAN 73 **1473** EDITION OF 1 NOV 65 IS OBSOLETE

050 750

TABLE OF CONTENTS

3

LIST OF ILLUSTRATIONS

5

INTRODUCTION

In the late 1960's the aeronomy branch at the BRL needed the solutions to sets of stiff ordinary differential equations (ODES) that describe the positive and negative ion chemistry in the earth's D-region (~ 60-85 km). Adequate mathematical techniques for handling stiff ODES were unknown to us at that time. Kregel, a physicist, approached this problem empirically and developed a stiff ODE integrator. This report sketches the K-method of integration and provides a few examples of the uses of this integrator. Our aim is two-fold: to interest mathematicians so that this method may be placed on a firmer mathematical foundation and to inform potential users so that they may apply this algorithm to their particular problem.

TWO BASIC PROBLEMS

Before we discuss the sketch and the examples let us briefly review two problems that are basic to any numerical solution to ODES, stiff or not. These problems are truncation error and stability. According to Dahlquist and Björck,[1] ..."(truncation errors) are committed when a limiting process is broken off before one has come to the limiting value." Truncation errors result from mathematical approximations. For example they arise when a finite series approximates an infinite series or when a linear function approximates a non-linear one.

Stability, or its better known opposite, instability, is associated with the idea of feedback.[2] As the name implies, part of a program or code has a loop in which the numbers produced at the output of one cycle are used as the input for the next cycle. The errors associated with these numbers may then be amplified in such a way as to destroy the solution.

The purpose in recalling these nemeses is to justify the effort that has gone into the K-method algorithm to reduce truncation error and to maximize stability consistent with a reasonable execution time.

---

[1] Numerical Methods, by G. Dahlquist and A. Björck, Trans. by N. Anderson, 1974, Prentice-Hall, Inc., Englewood Cliffs, NJ, p. 22.

[2] See for example Numerical Methods for Scientists and Engineers, by R. W. Hamming, 2nd Edition, 1973, McGraw-Hill, Inc. p. 5.

SKETCH OF THE K-METHOD

Figure 1 schematically shows the main functional steps in the K-method algorithm.[3] A third-order predictor-corrector method is employed. As soon as the initial corrector is formed, the diagonal of the Jacobian (i.e. $\partial y_i'/\partial y_i$) is examined to determine those dependent variables that are stiff and those that are not (not shown in Fig. 1). This is done in order to select the method with the least computational overhead for updating each of the initial predictor values.

At this stage of the algorithm neither the predictor values nor corrector values are presumed acceptable and an error vector is generated from their difference. This vector, in conjunction with the Jacobian including, now, the off-diagonal elements, is used to modify the predictor values. The modifications to the predicted values, which involve a matrix inversion, are first attempted iteratively using a Gauss-Seidel method. During the iteration, checks are made on the estimated computational overhead burden. Should the iteration method prove too tedious, the remaining "non-converged" correction elements are solved by direct matrix inversion. The corrector is recomputed and another error vector is generated.

Truncation error is then checked by comparing the fourth derivative of each dependent variable against a predetermined relative error tolerance. If any one of these variables fails this test, the truncation error is judged "poor," the step size, h, is reduced by a factor of two and this cycle of the computation is begun anew. This test is especially useful, as we shall see later, in the case of discontinuous driving functions.

When all the dependent variables have passed the truncation test, (i.e., are "OK" in Fig. 1) a check is made on the predictor-corrector agreement. Should all elements of the predictor-corrector difference vector be less than a predetermined minimum error (i.e. are "OK"), the corrector values are accepted as the solutions at this time step and the step size is adjusted for the next cycle. If any element of this difference vector is greater than a predetermined maximum error tolerance the agreement is judged "poor," the step size is reduced by a factor of two and this cycle begun anew. For the intermediate case, in which all elements of this difference vector are less than the maximum error test, and in which at least one is greater than the minimum error test, the difference vector is judged "so-so." When this is the case the predicted values are again modified and the process begun anew until an acceptable

---

[3] An earlier version has been reported. See "Description and Comparison of the K-Method for Performing Numerical Integration of Stiff Ordinary Differential Equations," by M. D. Kregel and E. L. Lortie, BRL Report No. 1733, July 1974, AD #A003855.

ENTER

PREDICT

CORRECT

h → h/2

MODIFY PREDICTOR VALUES

RECOMPUTE CORRECTOR VALUES

TEST FOR

POOR ← • TRUNCATION ERROR

↓ OK

POOR ← • PREDICTOR - CORRECTOR AGREEMENT   SO - SO
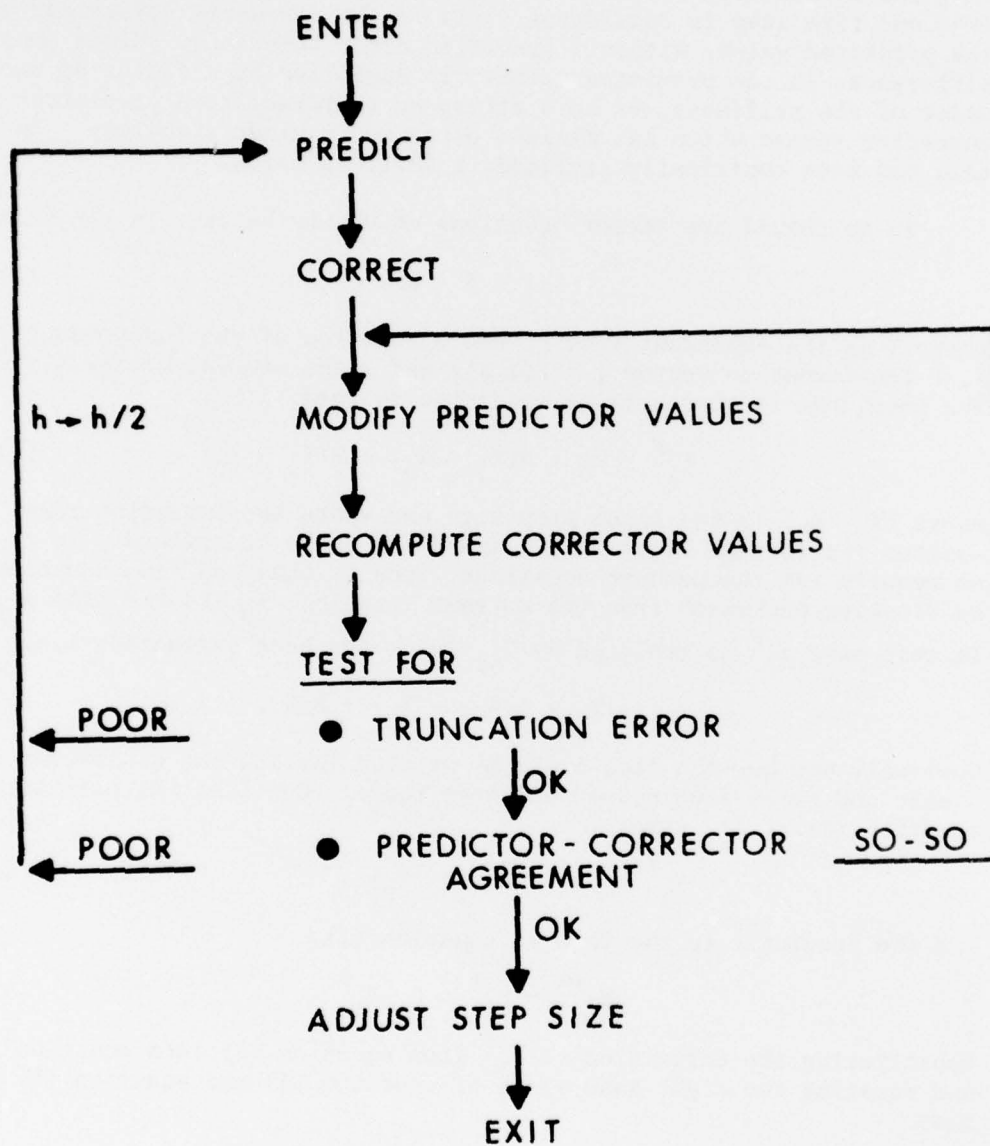
↓ OK

ADJUST STEP SIZE

EXIT

Figure 1.   Schematic of K-method of integration; h is the step size.

9

solution is obtained. It is important to note that the K-method conserves both charge, if any, and chemical balance to within the round-off error of the machine since the corrector formulation itself is conservative.

The methodology outlined in Figure 1 and above shows that a solution over one time step is considered valid if the corrected values map into the predicted values within a specified error tolerance. Since small differences in the predicted values are magnified by a factor of the order of the stiffness, we have attempted to formulate a predictor-corrector scheme which has minimum error and maximum stability. How this has been empirically achieved is outlined below.

To be solved are vector equations which may be cast in the form of

$$Y' = F - RY, \tag{1}$$

where Y is the dependent vector, and a function of the independent variable X, F the formation vector [= $F(Y,X)$] and R the removal vector [= $R(Y,X)$]. The predictor is chosen to be quadratic in form; i.e.,

$$Y_1^P = Y_0 + A(X_1 - X_0) + B(X_1 - X_0)^2, \tag{2}$$

where $(X - X_0)$ is the local step size and where the subscript zero denotes the current location. A and B are to be determined. To do this we require two independent equations. One is obtained from equation (2) by "looking backward" from the current location, X_0, to the time X_{-1}. In this case Y_1^P is replaced by Y_{-1} which has been evaluated, i.e.,

$$Y_{-1} = Y_0 + A(X_{-1} - X_0) + B(X_{-1} - X_0)^2 . \tag{3}$$

Obviously another equation could be written for Y_{-2} but an alternate, more stable and error-free method has been found. Consider the derivative of equation (2) at X_1, namely,

$$Y_1^{P'} = A + 2B(X_1 - X_0) , \tag{4}$$

and the predictor in the form of equation (1),

$$Y_1^{P'} = F_1^P - R_1^P Y_1^P . \tag{5}$$

Substituting the definition of Y_1^P from equation (2) into equation (5) and equating the right hand sides of equation (4) and equation (5) we have

$$A + 2B(X_1 - X_0) = F_1^P - R_1^P[Y_0 + A(X_1 - X_0) + B(X_1 - X_0)^2]. \tag{6}$$

Provided F_1^P and R_1^P are known, equation (6) provides the second equation required to determine A and B.

10

Let us now consider how F_1^P and R_1^P are determined. Figure 2 shows the current and three previous discrete values of the formation element for a given dependent variable. A parabola of the form

$$F(X) = C_1 + C_2(X - X_0) + C_3(X - X_0)^2 , \qquad (7)$$

is passed through these four points. The C_j's (j=1,2,3) of equation (7) are found from a least squares fit where the function to be minimized with respect to the C_j is

$$\sum_i W_i [F_i - F(X_i)]^2, \quad -3 \leq i \leq 0 . \qquad (8)$$

The W_i are weighting functions, chosen so that periodic fluctuations in the F_i values will not propagate into F_1^P. (The relative weights are determined by adding a quantity $\alpha(-1)^i$ to each of the four F_i and requiring that the identical F_1^P be found.) R_1^P is found in a similar fashion. Once F_1^P and R_1^P are determined, A and B can be determined, and consequently, Y_1^P.

The corrector is given by

$$Y_1^C = A_2 Y_{-2} + A_1 Y_{-1} + A_0 Y_0 + (X_1 - X_0)(DY_{-1}' + BY_0' + CY_1^{P'}), \quad (9)$$

where D and B are preselected to minimize both truncation error and noise amplification, and to maximize relative stability. Values for the coefficients in equation (9) can be found in Reference 3.

EXAMPLES

We shall now consider three examples of the types of problems the K-method has been called upon to handle. They are all drawn from the field of aeronomy. Figure 3 shows a linear plot of a piecewise continuous driving function [Q(t), solid line]. The discontinuities are instantaneous since they were formed by reading from a DATA block with (J) and (J + 1) subscripts interchanged. (The reverse of each of the slopes in Figure 3 gives the desired driving function, which is still discontinuous in the first derivative.) The dashed lines are the response of the electron density and a primary positive ion density, here the nitric oxide ion, as a function of time. The curves have been vertically displaced for ease in reading. It is seen that the K-method enables the dependent variables to follow the input discontinuities of the driving term. (Departures from a perfect matching of the input slopes can be explained by chemistry competing with the driving term.) This example demonstrates the effect of careful monitoring of the truncation error.

11

Figure 2. Schematic of a parabolic fit to the values of F at the current and three previous times for one of the dependent variables. F_1^P is found by continuing this parabola to the time X_1.
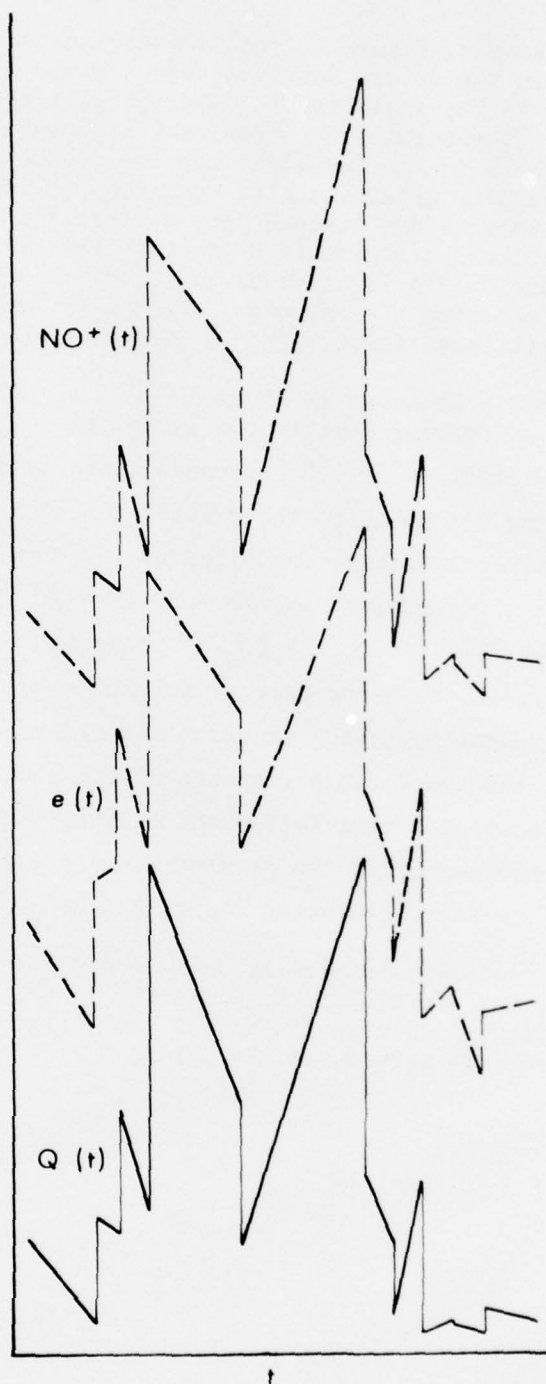
Figure 3. The driving function, Q(t) (solid line) and the response of two primary charged particle densities (dashed lines) are shown as a function of time, t. Abscissa is linear with dimensions ion-pairs $cm^{-3} s^{-1}$ for Q(t) and cm^{-3} for both e(t) and $NO^+(t)$. Curves have been vertically displaced for ease in reading.

The second example, Figure 4, shows histograms of the number of species that lie in the decade interval, h/τ_i, where h is the local step size and where τ_i is the instantaneous characteristic time constant of the ith species.[1] (The total area under each histogram corresponds to 64 species.) The numbers to the far right are the decade model times in seconds (i.e., computer execution time runs from bottom to top in this figure). The histograms are divided into a stiff segment to the right of the dashed line, and a non-stiff segment to the left. On the first plot (10^{-5} seconds) only a few species are stiff while at the upper limit of this integration (10^3 seconds) the number has significantly increased, with stiffness factors (h/τ_i) greater than 10^7.

The last example is shown in Figures 5 and 6. Figure 5 shows the log of the input or driving function, q(e), plotted against the log of time. In the interval 10^{-4} - 10^{-2} seconds those negatively charged species more strongly coupled to the driving function, (e.g. e, O_2^- or O_3^-) follow the discontinuities exhibited by the driving term. These details tend to be "washed-out" in the species that are weakly coupled to the driving term (e.g. CO_3^- or CO_4^-). Near 10^2 seconds the strongly coupled species again track the discontinuities in q(e). The dynamic range in the dependent variables is about six orders of magnitude. Figure (6) shows the broad range response of the neutral species. This graph shows those species that follow the driving term [e.g. $O(^1D)$, $N(^2D)$], those that are independent of the driving term [e.g. N_2O, CO] and those that tend to be chemistry dominated [e.g. H_2, HNO_2, N_2O_5].

In summary, we have empirically derived a third order, variable step size method for efficiently handling stiff ODES that appears to work for discontinuous driving functions. We anticipate with some further work that this method will be put on a firmer mathematical foundation.

14
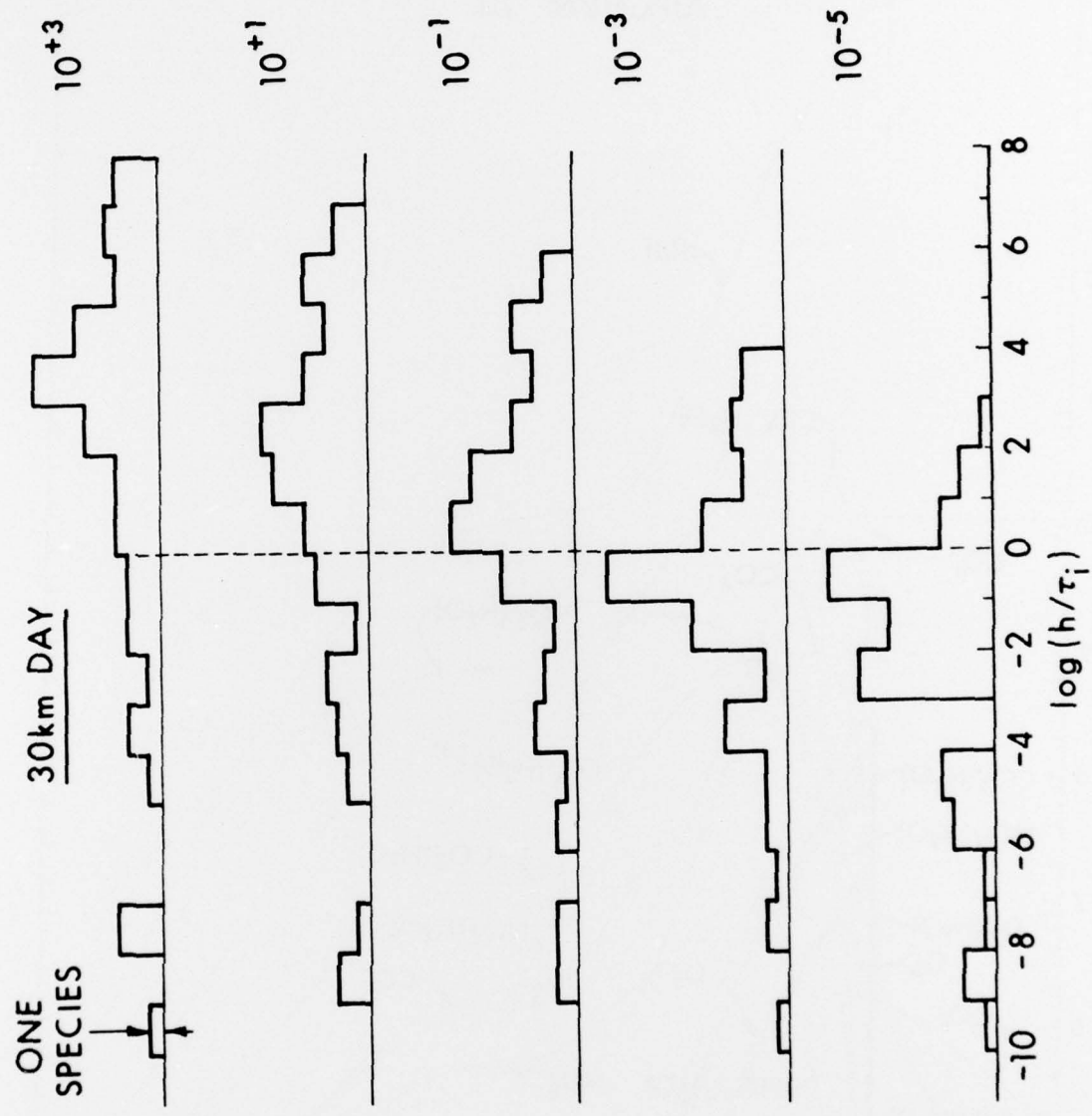
Figure 4. Histograms that characterize the stiffness of chemical species found in a daytime deionization model of the atmosphere at an altitude of 30 km. (See text for details).
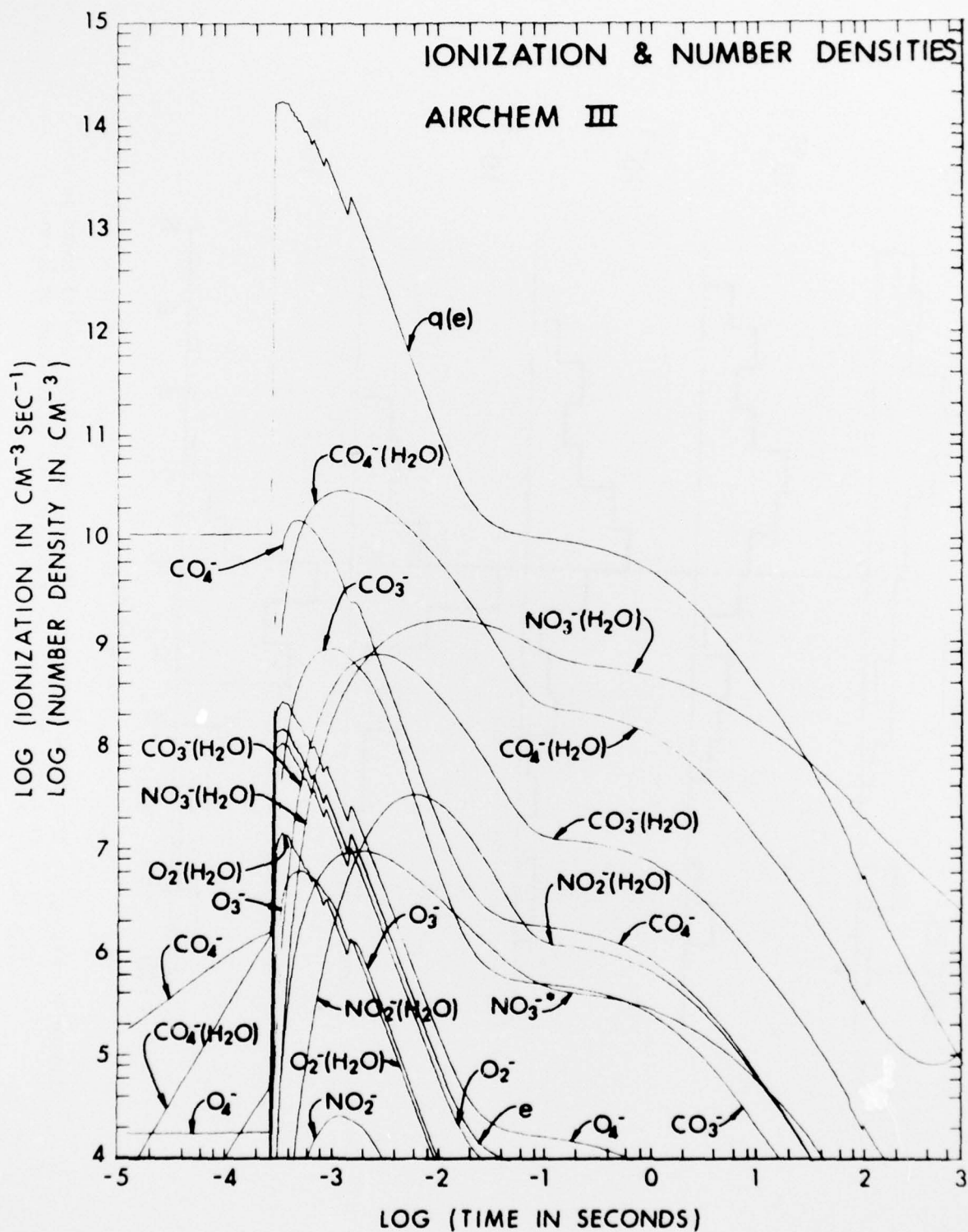
Figure 5. Modeled response of the negative ion densities to the driving function q(e).
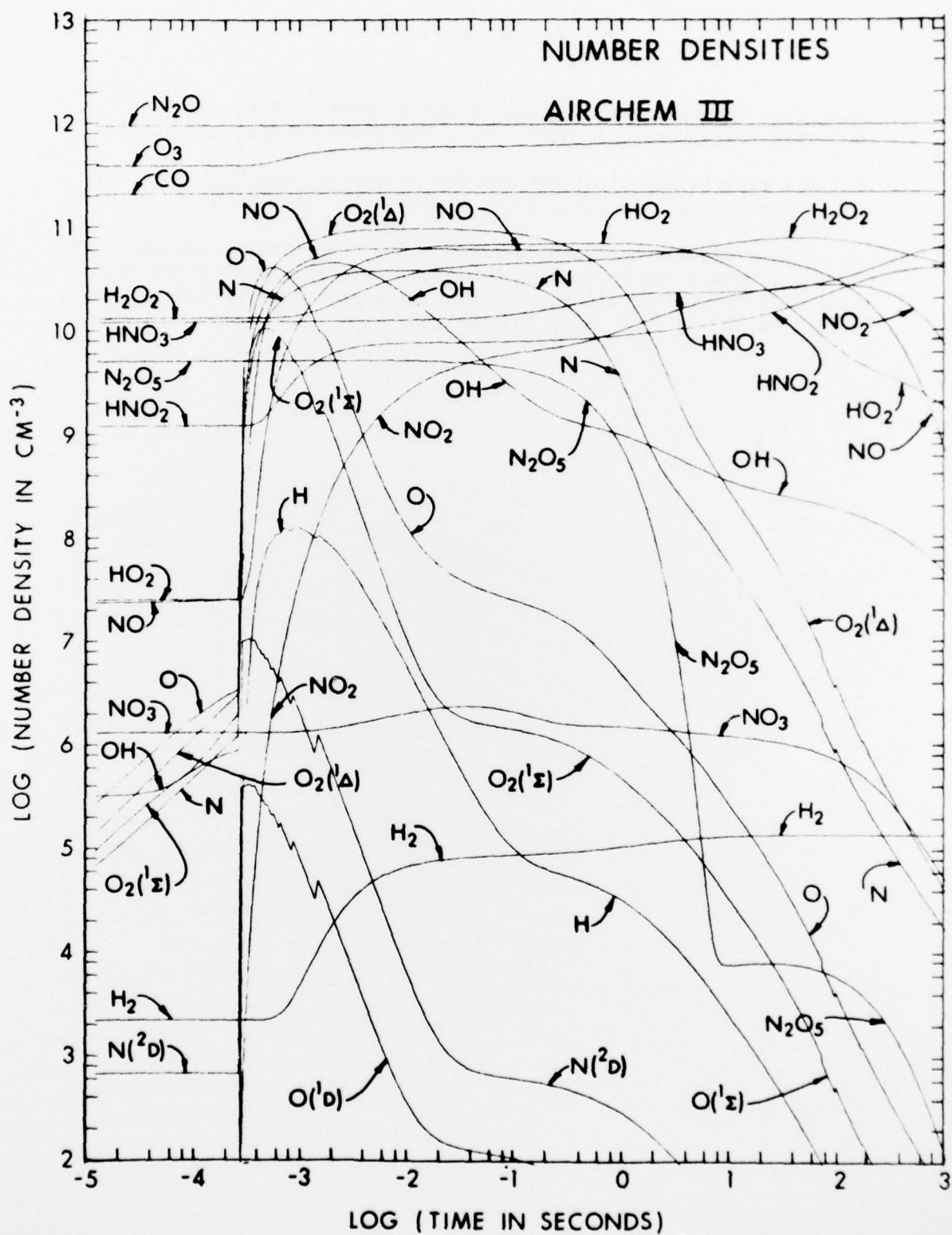
Figure 6. Modeled response of the neutral densities to the same
driving function of Fig. 5.

REFERENCES

1. Numerical Methods, by G. Dahlquist and A. Björck, Trans. by N. Anderson, 1974, Prentice-Hall, Inc., Englewood Cliffs, NJ, p. 22.

2. See for example Numerical Methods for Scientists and Engineers, by R. W. Hamming, 2nd Edition, 1973, McGraw-Hill, Inc. p. 5.

3. An earlier version has been reported. See "Description and Comparison of the K-Method for Performing Numerical Integration of Stiff Ordinary Differential Equations," by M. D. Kregel and E. L. Lortie, BRL Report No. 1733, July 1974, AD #A003855.

DISTRIBUTION LIST

No. of Copies	Organization	No. of Copies	Organization
12	Commander Defense Documentation Center ATTN: DDC-TCA Cameron Station Alexandria, VA 22314	1	Director Defense Communications Agency ATTN: Code 340, Mr. W. Dix Washington, DC 20305
1	Director Institute for Defense Analyses ATTN: Dr. E. Bauer 400 Army-Navy Drive Arlington, VA 22202	1	Commander US Army Materiel Development and Readiness Command ATTN: DRCDMA-ST 5001 Eisenhower Avenue Alexandria, VA 22333
2	Director Defense Advanced Research Projects Agency ATTN: STO, CPT J. Justice, Dr. S. Zakanyca 1400 Wilson Boulevard Arlington, VA 22209	1	Commander US Army Aviation Research and Development Command ATTN: DRSAV-E 12th and Spruce Streets St. Louis, MO 63166
2	Director of Defense Research and Engineering ATTN: Mr. D. Brockway CAPT K. Ruggles Washington, DC 20305	1	Director US Army Air Mobility Research and Development Laboratory Ames Research Center Moffett Field, CA 94035
4	Director Defense Nuclear Agency ATTN: STAP (APTL) STRA (RAAE) Dr. C. Blank Dr. H. Fitz, Jr. DDST Washington, DC 20305	1	Commander US Army Electronics Command ATTN: DRSEL-RD Fort Monmouth, NJ 07703
2	DASIAC/DOD Nuclear Information and Analysis Center General Electric Company-TEMPO ATTN: Mr. A. Feryok Mr. W. Knapp 816 State Street P.O. Drawer QQ Santa Barbara, CA 93102	6	Commander/Director US Army Electronics Command Atmospheric Sciences Laboratory ATTN: Dr. E. H. Holt Mr. N. Beyers Mr. F. Horning Dr. F. E. Niles Dr. M. G. Heaps Dr. D. E. Snider White Sands Missile Range, NM 88002

DISTRIBUTION LIST

No. of Copies	Organization

1 Commander
US Army Missile Research
    and Development Command
ATTN: DRDMI-R
Redstone Arsenal, AL 35809

1 Commander
US Army Tank Automotive
    Development Command
ATTN: DRDTA-RWL
Warren, MI 48090

1 US Army Mobility Equipment
    Research & Development Command
ATTN: Tech Docu Cen, Bldg. 315
        DRSME-RZT
Fort Belvoir, VA 22060

1 Commander
US Army Armament Materiel
    Readiness Command
Rock Island, IL 61202

1 Commander
US Army Armament Research
    and Development Command
Dover, NJ 07801

1 Commander, USACEEIA
ATTN: CCC-CED-EMED (Miles Merkel)
Fort Huachuca, AZ 85635

2 Commander
US Army Harry Diamond Labs
ATTN: DRXDO-TI
        DRXDO-NP, Mr. F. Wimenitz
2800 Powder Mill Road
Adelphi, MD 20783

1 Director
US Army TRADOC Systems
    Analysis Agency
ATTN: ATAA-SA
White Sands Missile Range
NM 88002

1 Commander
US Army Nuclear Agency
ATTN: Dr. J. Berberet
Fort Bliss, TX 79916

3 Commander
US Army Research Office
ATTN: Dr. A. Dodd, Dr. D. Squire
        Dr. R. Lontz
P.O. Box 12211
Research Triangle Park, NC 27709

2 Director
US Army BMD Advanced Technology
    Center
ATTN: Mr. M. Capps
        Mr. W. Davies
P.O. Box 1500
Huntsville, AL 38507

2 Commander
US Army BMD System Command
ATTN: SSC-HS, Mr. H. Porter
        SSC-TET, Mr. E. Carr
P.O. Box 1500
Huntsville, AL 35807

1 Director
US Army Ballistic Missile
    Defense Program Office
ATTN: Mr. C. McLain
5001 Eisenhower Avenue
Alexandria, VA 22333

1 HQDA (DAEN-RDM/Dr. F. de Percin)
Washington, DC 20314

3 Commanding Officer
US Army Research & Development
    Group (Europe)
ATTN: Dr. H. Lemons,
        Dr. G. R. Husk,
        LTC J. Kennedy
Box 15
FPO New York 09510

DISTRIBUTION LIST

No. of Copies	Organization	No. of Copies	Organization
1	Chief of Naval Research ATTN: Code 418, Dr. J. Dardis Department of the Navy Washington, DC 20360	2	Sandia Laboratories ATTN: Dr. K. J. Touryan Dr. F. Hudson P.O. Box 5800 Albuquerque, NM 87115
1	Commander US Naval Surface Weapons Center ATTN: Dr. L. Rutland Silver Spring, MD 20910	1	Director National Aeronautics and Space Administration Goddard Space Flight Center ATTN: Dr. R. Goldberg (Code 912) Greenbelt, MD 20771
1	Commander US Naval Electronics Laboratory ATTN: Mr. W. Moler San Diego, CA 92152	2	Director National Bureau of Standards US Department of Commerce ATTN: R. F. Hampson Dr. Richard Kraft, Div. 205.01 Washington, DC 20234
4	Commander US Naval Research Laboratory ATTN: Dr. W. Ali Dr. D. Strobel Code 7700, Mr. J. Brown Code 2020, Tech Lib Washington, DC 20375	2	Director National Science Foundation ATTN: Dr. F. Eden Dr. G. Adams 1800 G. Street, N.W. Washington, DC 20550
4	HQ USAF (AFNIN; AFRD; AFRDQ/ ARTAC/COL C. Anderson) Washington, DC 20330	1	Boeing Computer Services, Inc. Energy Technology Applications ATTN: Dr. Kenneth W. Neves P.O. Box 24346 Seattle, WA 98124
2	AFGL (LKB, Dr. K. Champion, Dr. W. Swider) Hanscom AFB, MA 01730	1	Calspan Corporation ATTN: Mr. R. Fluegee P.O. Box 235 Buffalo, NY 14221
2	AFSC (DLCAW, LTC R. Linkous; SCS) Andrews AFB, 20334	2	General Electric Company Valley Forge Space Technology Center ATTN: Dr. M. Bortner Dr. T. Baurer P.O. Box 8555 Philadelphia, PA 19101
4	Director Los Alamos Scientific Laboratory ATTN: Dr. W. Maier (Gp J-10) Dr. J. Zinn (MS 664) Dr. W. Myers Dr. M. Peek P.O. Box 1663 Los Alamos, NM 87544		

DISTRIBUTION LIST

No. of Copies	Organization	No. of Copies	Organization
1	General Research Corporation ATTN: Dr. J. Ise P.O. Box 3587 Santa Barbara, CA 93105	1	Science Applications, Inc., Huntsville ATTN: Mr. R. Byrn 2109 West Clinton Avenue Suite 100 Huntsville, AL 358051
2	Lockheed Palo Alto Research Laboratory ATTN: Dr. J. Reagan Mr. R. Sears 3251 Hanover Street Palo Alto, CA 94304	1	Spectra Research Systems, Inc. ATTN: Mr. B. Kilday 2212 Dupont Drive Irvine, CA 92664
1	Mission Research Corporation ATTN: Dr. M. Scheibe 735 State Street P.O. Drawer 719 Santa Barbara, CA 93102	2	Stanford Research Institute ATTN: Dr. J. Peterson Dr. D. Golden 333 Ravenswood Avenue Menlo Park, CA 94025
1	Mitre Corporation ATTN: Tech Lib P.O. Box 208 Bedford, MA 01730	1	Systems Control, Inc. ATTN: Mr. R. Foerster 260 Sheridan Avenue Palo Alto, CA 94306
1	Pacific-Sierra Research Corp. ATTN: Mr. E. Fields 1456 Cloverfield Blvd. Santa Monica, CA 90404	1	Systems, Science & Software ATTN: Dr. R. Englemore P.O. Box 1620 La Jolla, CA 92037
1	R&D Associates ATTN: Dr. F. Gilmore P.O. Box 9695 Marina Del Rey, CA 90291	1	TRW Systems Group ATTN: Tech Lib One Space Park Redondo Beach, CA 90278
1	The Rand Corporation ATTN: Dr. C. Crain 1700 Main Street Santa Monica, CA 90406	1	Visidyne, Inc. ATTN: Dr. H. Smith 19 Third Avenue, N.W. Industrial Park Burlington, MA 01803
2	Science Applications, Inc. ATTN: Mr. R. Lowen, Mr. D. Hamlin 1250 Prospect Plaza La Jolla, CA 90406	1	Purdue University Indianapolis Regional Campus ATTN: Dr. John M. Gersting 1201 East 38th Street Indianapolis, IN 46205

DISTRIBUTION LIST

No. of
Copies   Organization

1   University of California
    Electrical Engineering and
      Computer Science Department
    ATTN: Prof. W. Kahan
    567 Evans Hall
    Berkeley, CA 94720

1   University of Illinois
    Department of Electrical Engineering
    ATTN: Dr. C. Sechrist, Jr.
    Urbana-Champaign Campus
    Urbana, IL 61801

1   University of Minnesota, Morris
    Division of Science and Mathematics
    ATTN: Dr. M. N. Hirsh
    Morris, MN 56267

1   University of Texas at El Paso
    Physics Department
    ATTN: Ms. J. Collins
    El Paso, TX 79902

1   University of Wisconsin - Madison
    Mathematics Research Center
    ATTN: Dr. Dennis C. Jespersen
    610 Walnut Street
    Madison, WI 53706

1   Utah State University
    Center for Research in Aeronomy
    ATTN: Dr. L. Megill
    Logan, UT 84321

1   Wayne State University
    Department of Engineering
    ATTN: Dr. R. Kummler
    Detroit, MI 48202

Aberdeen Proving Ground

    Marine Corps LnO
    Dir, USAMSAA